Methods

CAR T cell manufacturing and chronic stimulation cultures

Lentiviral vectors were manufactured as previously described.[9] PBMCs were procured from Miltenyi Biotec and CD4 and CD8 cells were purified using magnetic beads (Miltenyi Biotec) and combined at a 1:1 ratio. T cells were activated using CD3/CD28 stimulatory beads (DynaBeads; Thermo-Fisher) at a ratio of 3 beads/cell and incubated at 37°C overnight. The following day, CAR lentiviral vectors were added to stimulatory cultures at a MOI of 2-4. Beads were removed after 6 day of stimulation, and cells were counted daily until growth kinetics and cell size demonstrated they had rested from stimulation. For all studies described, CAR constructs also encoded a truncated CD34 (tCD34) surface marker of transduction, separated from the CAR transgene by a P2A sequence. Both CD28 and 41BB-based CARs were composed of the FMC63 single chain variable fragment targeting CD19, CD8α hinge and transmembrane regions, followed by a costimulatory domain and a terminal CD3ζ signaling domain.

General cell culture and flow cytometry

Unless otherwise specified, cells were grown and cultured at a concentration of $1x10^6$ cells/mL of standard culture media (RPMI 1640 + 10% FCS, 1% penicillin/streptomycin, 1% HEPES, 1% non-essential amino acids) at 37°C in 5% ambient CO_2. All co-culture studies were performed at an effector cell to target cell ratio of 1:8, unless otherwise stated. Samples were stained with CD34 (BD, clone 581, #555824), CD4 (Biolegend, clone OKT4, #317444), CD8 (Invitrogen, clone SK1, #17-0087-42), PD1 (Biolegend, clone eh12.2h7, #329928), TIM3 (Invitrogen, clone F38-2E2, #17-3109-42), LAG3 (Biolegend, clone 11c3c65, #369314), CD62L (Biolegend, clone dreg-56, #304822), CD45RO (Biolegend, clone UCHL1, #204236) and 7-AAD (BD, #559925) in 100ul FACS buffer (2%FBS in PBS), washed once with the same buffer and analyzed on the Attune NxT Flow Cytometer (ThermoFisher). GFP+ Nalm6 and GFP-CD34+ CAR T cells were gated and analyzed using FlowJo v9 or 10 (BD Biosciences).

CyTOF

Mass cytometry was performed as previously described.[12] Briefly, isolated CAR+ T cells were live/dead stained with a short pulse of cisplatin and surface stained for 30 minutes at room temperature. Cells were then washed and fixed overnight at 4°C with fix/perm buffer (eBiosciences). Intracellular staining was performed the following day at 4°C for 1 hour. Cells were barcoded according to manufacturer's instructions (Fluidigm). Cells were washed and suspended in PBS containing 2% paraformaldehyde with Cell-ID Intercalator-IR. Mass cytometry data was collected on a Helios mass cytometer and analyzed using Cytobank (Beckman Coulter).

Bulk RNA and ATAC sequencing and data analysis

RNA sequencing was performed on samples derived from 1 donor for day 0 samples and 4 donors for day 6 and 15 samples. Each assay was performed in technical triplicate and one sample from both day 15 samples was excluded due to poor RNA quality, resulting in n=3 samples at day 0, n=12 samples at day 6 and n=11 samples at day 15. Total RNA was extracted using Qiazol (Qiagen) and recovered by RNA Clean and Concentrator spin columns (Zymo). Samples were prepared according to library kit manufacturer's protocol, indexed, pooled, and sequenced on an Illumina NovaSeq 6000. Basecalls and demultiplexing were performed with Illumina's bcl2fastq2 software. RNA-seq reads were then aligned and quantitated to the Ensembl release 101 primary assembly with an Illumina DRAGEN Bio-IT on-premise server running version 3.9.3-8 software. All gene counts were then imported into the R/Bioconductor package EdgeR[13] and TMM normalization size factors were calculated to adjust for samples for differences in library size. The TMM size factors and the matrix of counts were then imported into the R/Bioconductor package Limma. Weighted likelihoods based on the observed mean-variance relationship of every gene and sample were then calculated for all samples and the count matrix was transformed to moderated log 2 counts-per-million with Limma's voomWithQualityWeights. Differential expression analysis was then performed to analyze for differences between conditions and the results were filtered for only those genes with Benjamini-Hochberg false-discovery rate adjusted p-values less than or equal to 0.05. Further analysis was performed using Partek Flow (Partek Inc). Geneset Enrichment Analysis was done using GSEA v4.1.0.

ATAC sequencing was performed on samples derived from 2 independent donors, also performed in technical triplicate resulting in n=6 samples for each time point. Omni ATAC-seq libraries were made as previously described.[14] Briefly, nuclei were isolated from 50,000 sorted CART19 cells, followed by the transposition reaction using Tn5 transposase (Illumina) for 30 minutes at 37°C with 1000rp mixing. Purification of transposed DNA was completed with DNA Clean and Concentrator (Zymo) and fragments were barcoded with ATAC-seq indices. Final libraries were double size selected using AMPure beads prior to sequencing. Paired-end sequencing (2 x 75 bp reads) was carried out on an Illumina NextSeq 500 platform. Adapters were trimmed using attack (version 0.1.5, https://atactk.readthedocs.io/en/latest/index.html), and raw reads were aligned to the GRCh37/hg19 genome using bowtie with the following flags: --chunkmbs 2000 --sam --best --strata -m1 -X 2000.[15] MACS2 was used for peak calling with an FDR cutoff of 0.05. Downstream analysis and visualization, including transcription factor motif analysis, was done using Partek Flow (Partek Inc).

Single cell RNA sequencing

CAR T cells from chronic stimulation cultures were isolated using flow-based sorting as described. For clinical samples, frozen vials of peripheral blood from a patient who underwent CAR T cell therapy and experienced a transient partial response followed by disease progression were gently thawed, counted, and dead cells were removed (Dead Cells Removal kit, Miltenyi, #130-090-101). Resulting cell samples had viabilities of 92-98% and were stained using an anti-FMC63 antibody (Acro Biochemicals, clone Y45, #FM3-HPY53) and then enriched for CAR+ cells using flow-based sorting. These cells were then processed using the 10x Genomics Chromium Single Cell V(D)J Reagent Kits (10x Genomics, PN-1000006, PN-1000020, PN-120262) to generate single-cell emulsions for barcoding, reverse transcription and cDNA amplification. Immediately following these steps, 10x barcoded fragments were pooled and attached to standard Illumina adaptors to generate a barcoded single-cell RNA library. Sequencing libraries were quantified by qPCR before sequencing on the Illumina platform using HiSeq 4000 instrument. Cell Ranger's count pipeline v6.1.1 (available at https://support.10xgenomics.com/single-cell-gene-expression/software/pipelines/latest/using/count) was applied to align reads and quantify gene expression of individual samples. Downstream single-cell analysis was performed using Seurat package v4.0.5 within the R programming environment v4.1.2.[16] Lower bound for the number of genes in individual cells was chosen based on binary logarithm distribution and was set to 9.8 for the dataset with chronic stimulation samples and 10.5 for the dataset with clinical samples. Additionally, cells with more than 7,500 genes for the dataset with chronic stimulation samples and 4,000 genes for the dataset with clinical samples were filtered out. The percentage of mitochondrial counts was calculated for every cell, and only cells with mitochondrial percentage less than 10% were used in further analysis. Filtered matrices were normalized using a scaling factor of 10,000 and centered. Two sources of unwanted variation, total number of counts and percentage of counts belonging to mitochondrial genes, were regressed using a linear model. Within the datasets samples were combined using the harmony batch correction function. UMAP dimensional reduction and shared nearest neighbor graph were calculated on harmony corrected PCA embeddings using 20 principal components. Number of principal components was selected based on the elbow plot. Graph-based clustering was performed on the reduced data. Differential expression analysis between clusters was performed using the MAST algorithm of Seurat R package[17], p value adjustment was done using Bonferroni correction. CD8+ T cells from the chronic stimulation dataset were processed with Monocle2 pseudotime analysis pipeline.[18] Seurat object were converted into CellDataSet object and used as an input. Differentially expressed genes between the clusters were identified with generalized linear model MAST, filtered by a significance level of p adjusted < 0.05 and used for cell ordering. Dimensionality reduction was performed with DDRTree method. The cells from the day 0 were set as the root of the trajectory. Single-cell regulatory network analysis was

performed with pySCENIC.[19,20] First, Seurat objects with raw filtered counts were converted into AnnData files via SaveH5Seurat and Convert functions from the SeuratDisk package (https://github.com/mojaveazure/seurat-disk/). Next, the adjacency matrix for transcription factors (hg38) and its targets were created using the GRNBoost2 algorithm.[21] Motif analysis was performed using the cisTarget database (https://resources.aertslab.org/cistarget/). Cellular enrichment for each regulon was calculated by the AUCell module[19] with default thresholds. Visualization and downstream analysis of pySCENIC output were performed with the SCopeLoomR package (https://github.com/aertslab/SCopeLoomR/).

T_{BBD} gene signature development

We determined which genes were biomarkers, or specifically enriched, in day 15 19/BB bulk RNA data and cluster 8 from scRNAseq data using Partek Flow. The overlap of each data set was used to generate the 145 gene signature. For these genes we developed a "contribution score" by multiplying the fold change of each gene relative to all other samples (5 samples from bulk RNAseq and 11 clusters for scRNAseq) from bulk and scRNAseq data. The 10 genes with the largest score were used for analysis in Figure 4e.

CRISPR/Cas9 gene editing

CRISPR sgRNAs were designed using the CRISPick tool from The Broad Institute and the sgRNA design tool from Integrated DNA Technologies (IDT). Cells were electroporated using the Lonza 4D-Nucleofector Core/X Unit. Triple Reporter Jurkat cells were electroporated using the SE Cell Line 4-D Nucleofector Kit, and primary T cells were electroporated using the P3 Primary Cell 4-D Kit (Lonza). For Cas9 and sgRNA delivery, a ribonucleoprotein (RNP) complex was first formed by incubating 5µg of TrueCut Cas9 Protein V2 (Lonza) with 10µg of sgRNA for 10 min at room temperature. Cells were washed twice with PBS (Gibco) and spun at 100xg for 10 min and resuspended at a concentration of 2-10x10^6 cells/100µL in the specified buffer. The RNP complex and 100µL of resuspended cells were combined and electroporated. Pulse codes EO-115 and CV-104 were used for resting primary T cells and Jurkat cells, respectively. After electroporation, the cells were incubated in standard 10% RPMI for Jurkat cells and cytokine enriched 10% RPMI (5 ng/ml IL7 and 5 ng/ml IL15, both from Peprotech) for primary T cells for the duration of experiment. Primary T cells were stimulated after 18 hours using CD3/CD28 Dynabeads (Thermo-Fisher) at 1:3 cell to bead ratio and engineered with lentivirus 24 hours later.

To determine efficiency of gene disruption, TIDE (Tracking of Indels by DEcomposition) analysis was used to detect knock out (KO) efficiency. Genomic DNA from electroporated cells was isolated (Qiagen

DNeasy Blood & Tissue Kit) and 100-200ng were PCR amplified using Q5 Hot Start High Fidelity 2x Master Mix (NEB) and 10μM forward/reverse primers flanking the region of interest. Primers were designed such that the amplicon was at a target size ~1 kb. PCR products were gel or column purified and sequenced, and trace files were analyzed using TIDE web tool (tide.nki.nl) to determine indel proportions. R^2 values were calculated, reflecting goodness of fit after non-negative linear modeling by TIDE software.[22]

Xenograft mouse models

6-10 week old NOD-SCID-$\gamma c^{-/-}$ (NSG) mice were obtained from the Jackson Laboratory and maintained in pathogen-free conditions. Animals were injected via tail vein with $1x10^6$ Nalm6 cells in 0.2mL sterile PBS. On day 7 after tumor delivery, either $0.125x10^6$ or $0.5x10^6$ CAR+ T cells (WT or *FOXO3*^{KO}) were injected via tail vein in 0.2mL sterile PBS. Animals were monitored for signs of disease progression and overt toxicity, such as xenogeneic graft-versus-host disease, as evidenced by >10% loss in body weight, loss of fur, diarrhea, conjunctivitis and disease-related hind limb paralysis. Disease burdens were monitored over time using the Xenogen IVIS bioluminescent imaging system, as previously described [9] and animals were sacrificed when radiance reached $>3x10^9$ photos/sec/cm2/sr (5-log greater than background). To avoid skewing of radiance data, graphical representation for each group was stopped after death of the first animal in the group.

Statistical analysis

All comparisons between two groups were performed using either a two-tailed unpaired Student's t-test or Mann-Whitney test, depending on normality of distribution. Comparisons between more than two groups were performed by two-way analysis of variance (ANOVA) with Bonferroni correction for multiple comparisons. All results are represented as mean ± standard error of the mean (s.e.m.). Survival data were analyzed using the Log-Rank (Mantel-Cox) test.

Supplementary Figure Legends

Supplementary Figure 1 | a, CAR expression in 19/28 and 19/BB after purification before co-culture (day 0) and after 15 days of chronic stimulation (day 15). **b,** Change in memory phenotype of CD4+ CAR T cell products after either acute (single combination with Nalm6 cells) or chronic stimulation. **c,** Activation of central T cell transcription factors in CAR Jurkat cells engineered to express a triple fluorescent reporter system. **d-e,** tSNE projection of **d,** 19/28 and **e,** 19/BB cells evaluated by CyTOF. Expression of **f,** PD1, **g,** TIGIT and **h,** CD62L in 19/28 and 19/BB cells.

Supplementary Figure 2 | a, PCA of RNAseq by donor (n=1 donor for day 0, n=4 donors for days 6 and 15). **b-c,** Volcano plot of DEGs at **b,** day 0 and **c,** day 6. **d,** KEGG pathways enriched in dysfunctional 19/28 and 19/BB cells. **e-h,** Overlap of genes with higher expression in 19/28 and 19/BB with previously published genesets defining exhausted tumor-infiltrating lymphocytes. Significance determined using Fisher's Exact Test. **i,** PCA of ATACseq by donor (n=2 donors).

Supplementary Figure 3 | a, Proportion of each sample (19/28 or 19/BB at day 0, 6 or 15) contained within each cluster. **b,** KEGG pathways enriched in each cluster.

Supplementary Figure 4 | a, Proportion of each CD8 cluster in day 15 samples. **b-c,** Expression of CD8 **b,** cluster 0 and **c,** cluster 1 markers in whole population analysis and in pseudotime analysis of CD8 cells.

Supplementary Figure 5 | Approach to generate a signature of 41BB-driven CAR T cell dysfunction. Genes that were uniquely upregulated in day 15 (dysfunctional) 19/BB cells by bulk RNAseq were compared to genes that were uniquely upregulated in cluster 8 from our scRNAseq dataset. Genes that were shared from these two lists were used to generate the 41BB dysfunction signature of 145 genes. Filtering to identify genes in both datasets was performed with $FDR < 0.05$ and $\log_2$-fold change >1.5.

Supplementary Figure 6 | a, Expression of *FOXP* transcripts over time. **b,** Expression of bZIP/AP1 factors over time. **c,** Enrichment of FOXO3 target genes in genes that marked identity of cluster 8. **d,** Expression of *FOXP3* transcripts over time in chronically stimulated 19/28 and 19/BB cells. **e,** Expression of *FOXP3* in scRNAseq of 19/28 and 19/BB cells collected at day 0, 6 and 15. Table on left represents $\log_2$-fold change (LFC) in expression of FOXP3 in each cluster that it is found to be enriched with associated false discovery rate (FDR).

Supplementary Figure 7 | a, Sequencing analysis of genomic *FOXO3* in CAR T cell manufacturing products demonstrating high-efficiency knockout. Performed using Synthego ICE. **b,** T cell expansion during manufacturing of 19/28 or **c,** 19/BB cells with genomic disruption of *FOXO3*. N=3 independent donors. **d,** Expansion of $FOXO3^{KO}$ or WT 19/28 or **e,** 19/BB CAR T cells during chronic stimulation. Representative data from n=3 independent donors. **f,** Western blot of lysates from CAR T cells engineered to overexpress FOXO3. **g,** T cell expansion during manufacturing of 19/28 and 19/BB with overexpression of FOXO3. N=2 independent donors. **h,** Expansion of $FOXO3^{OE}$ 19/28 or **i,** 19/BB CAR T cells during chronic stimulation. Representative data from n=2 independent donors. **j,** Expression of 7AAD by CAR+ T cells. **k,** CAR T cell size as measured by forward scatter area over the course of chronic stimulation. Representative data from n=3 independent donors. Statistical significance determined by two-tailed ANOVA with Bonferroni correction for multiple comparisons.

Supplementary Figure 8 | a, Nalm6 progression over time after treatment with $0.125x10^6$ CAR T cells or **b,** $0.5x10^6$ CAR T cells. Radiance curves were stopped at time of first animal death. Significance determined using two-way ANOVA. **c,** Individual animal radiance over time. For all studies n=5 animals per group.

Supplementary Figure 1

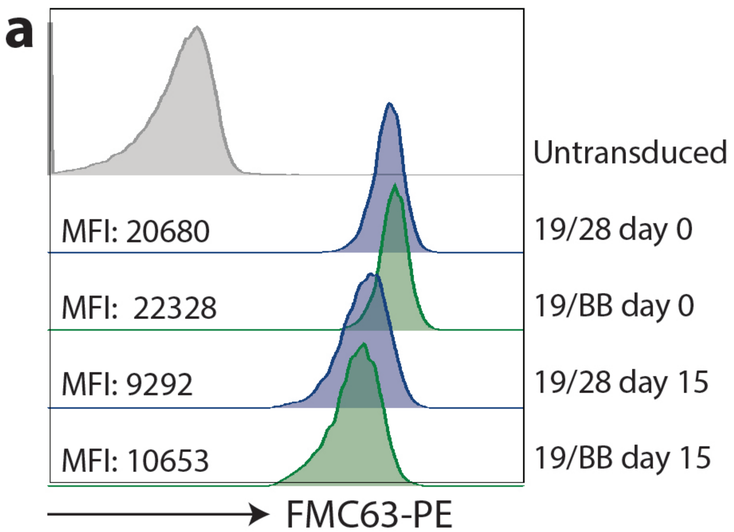

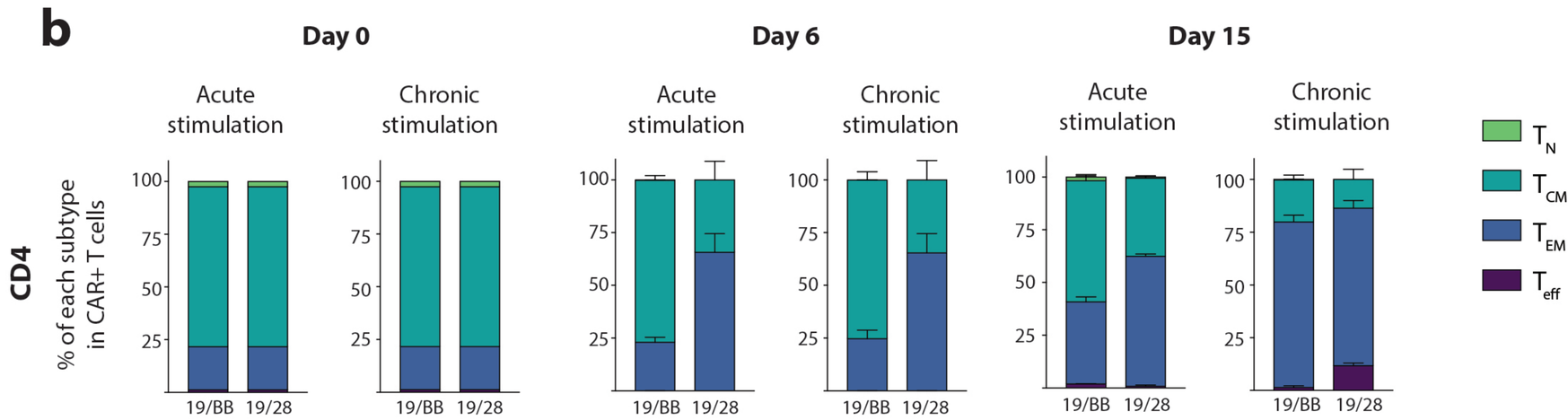

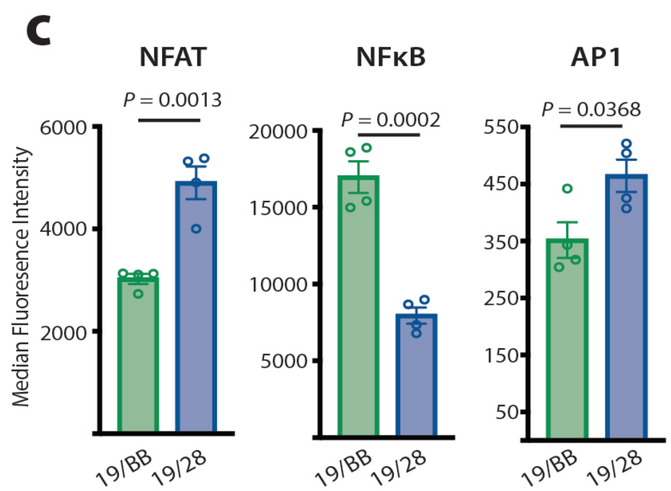

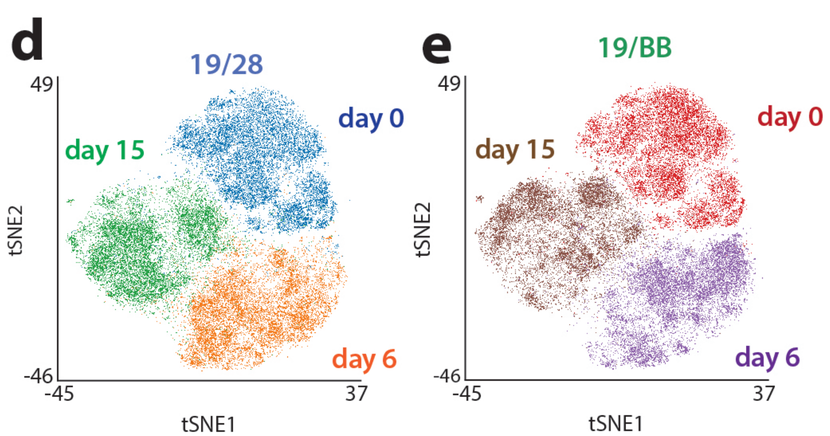

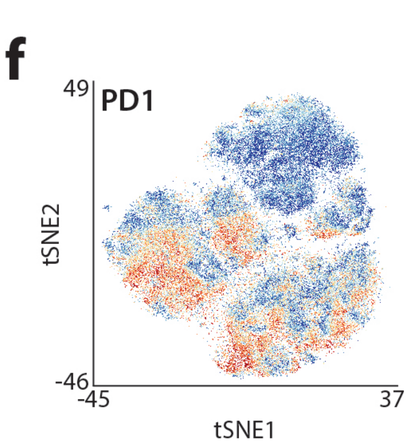

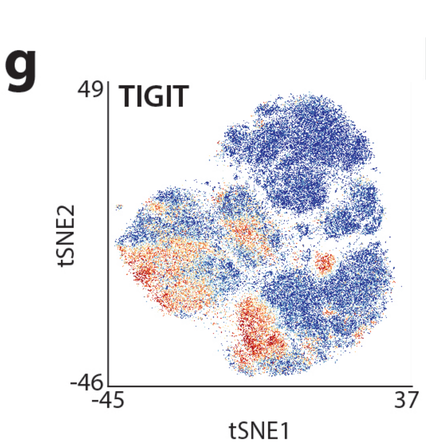

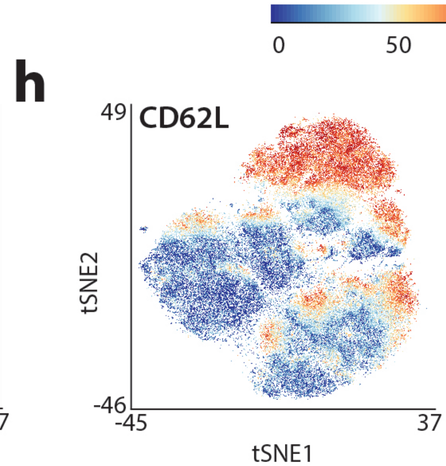

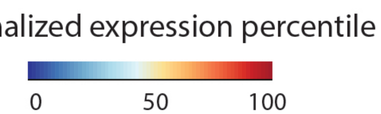

Supplementary Figure 2

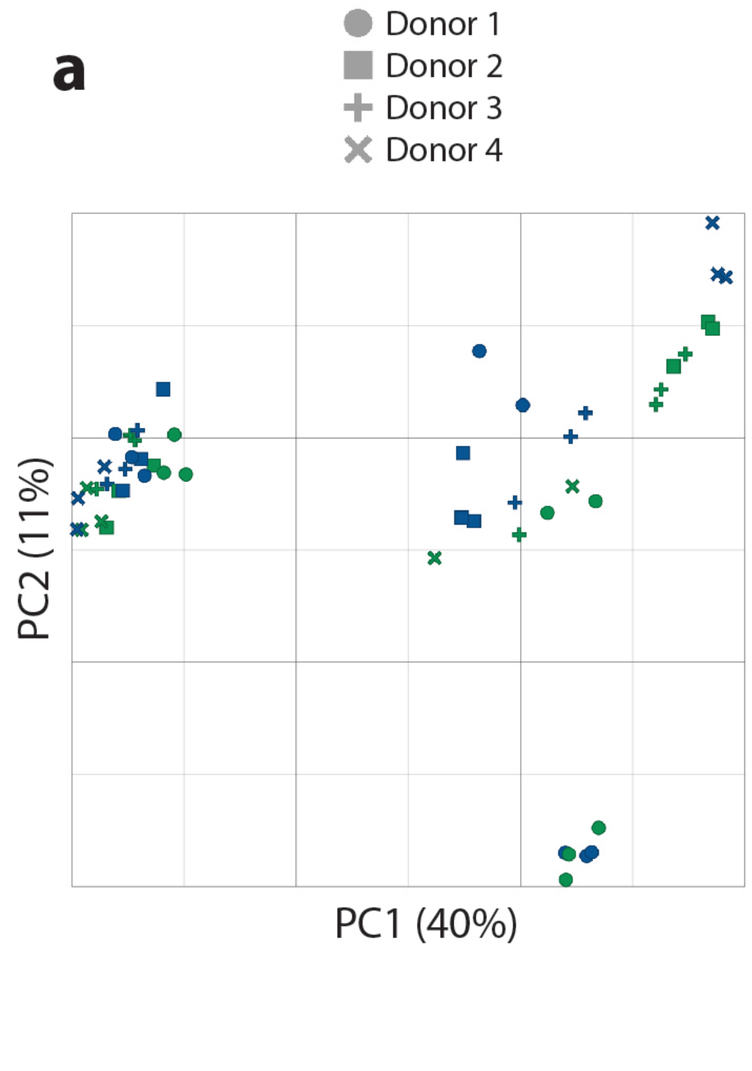

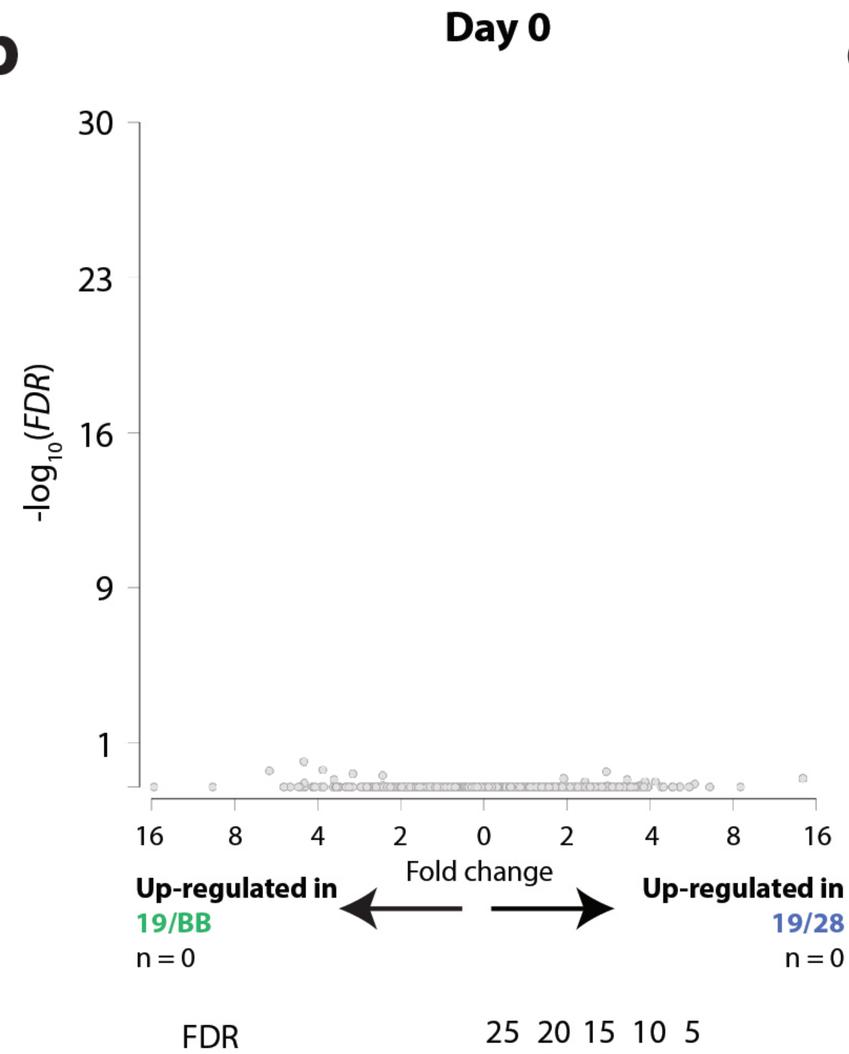

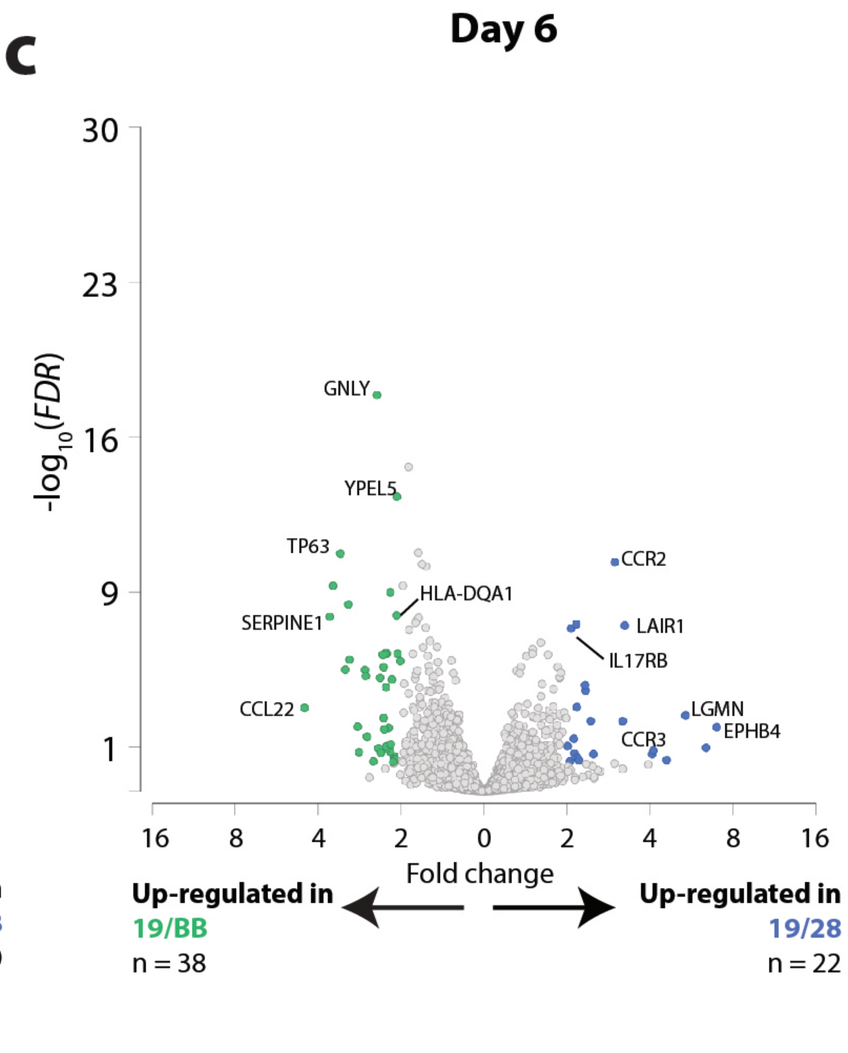

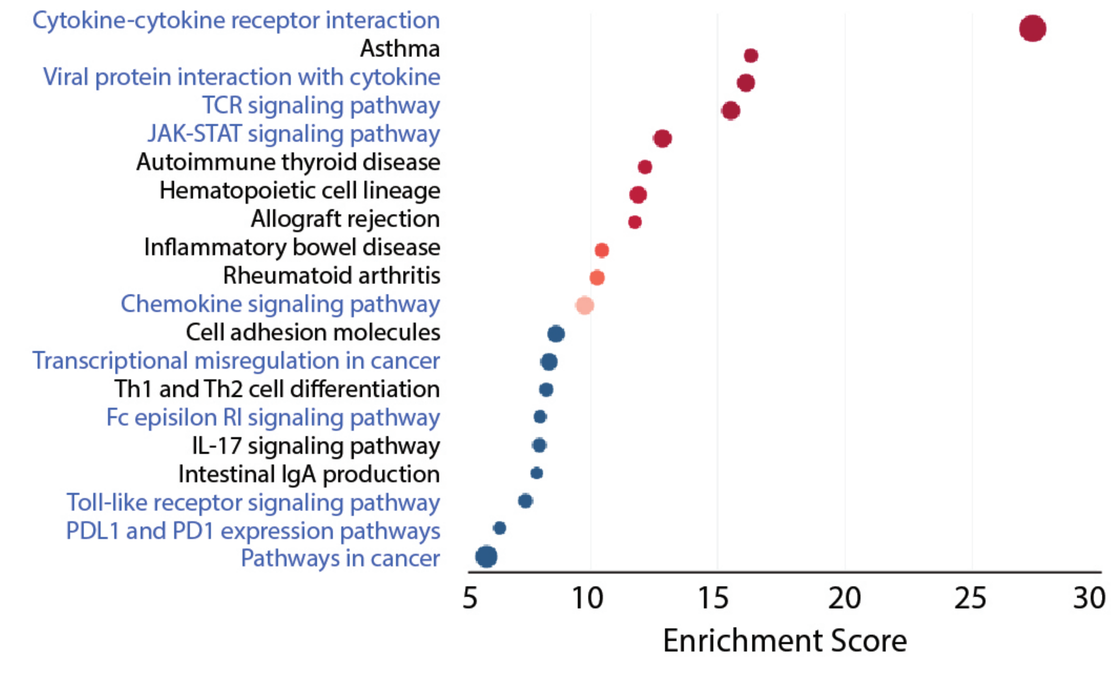

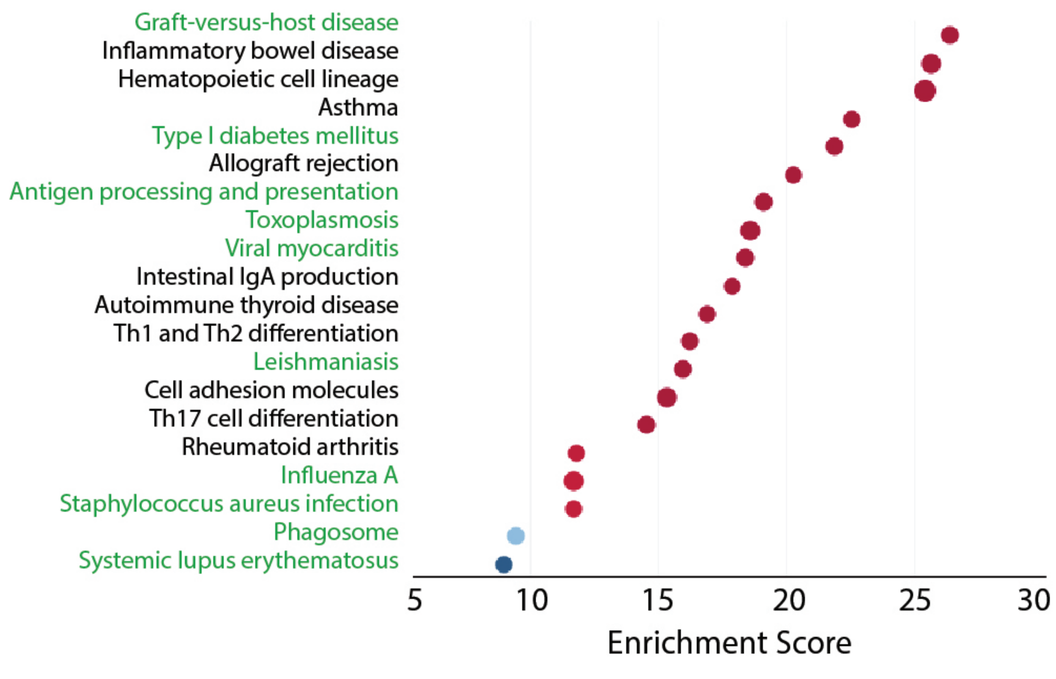

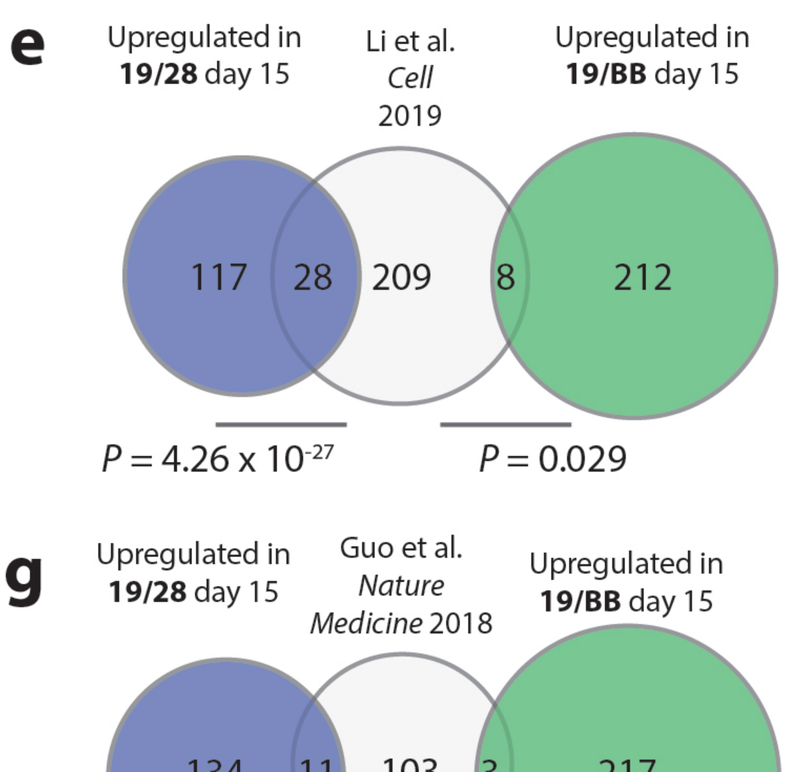

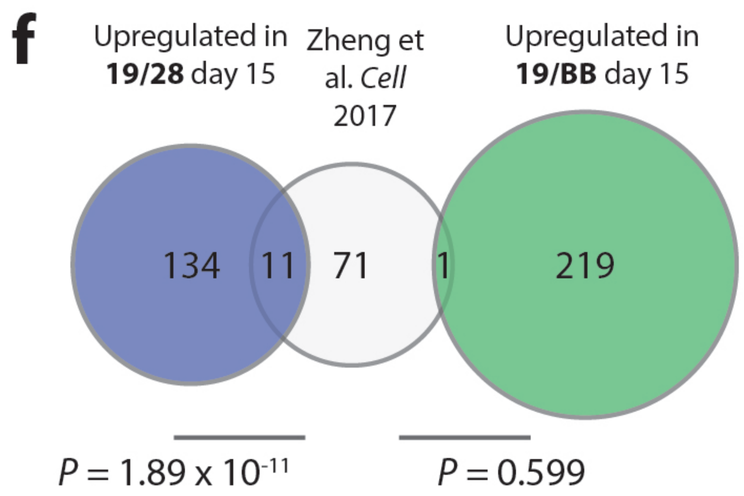

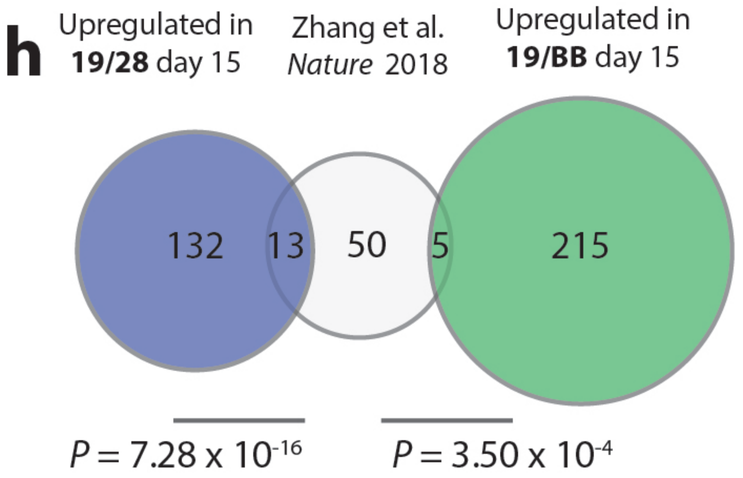

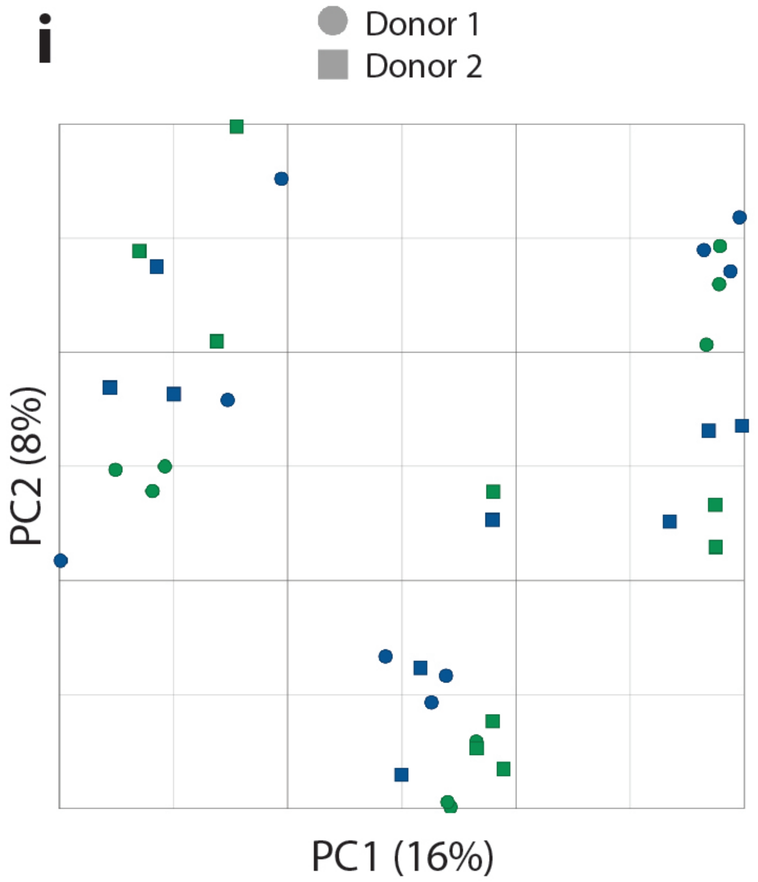

Supplementary Figure 3

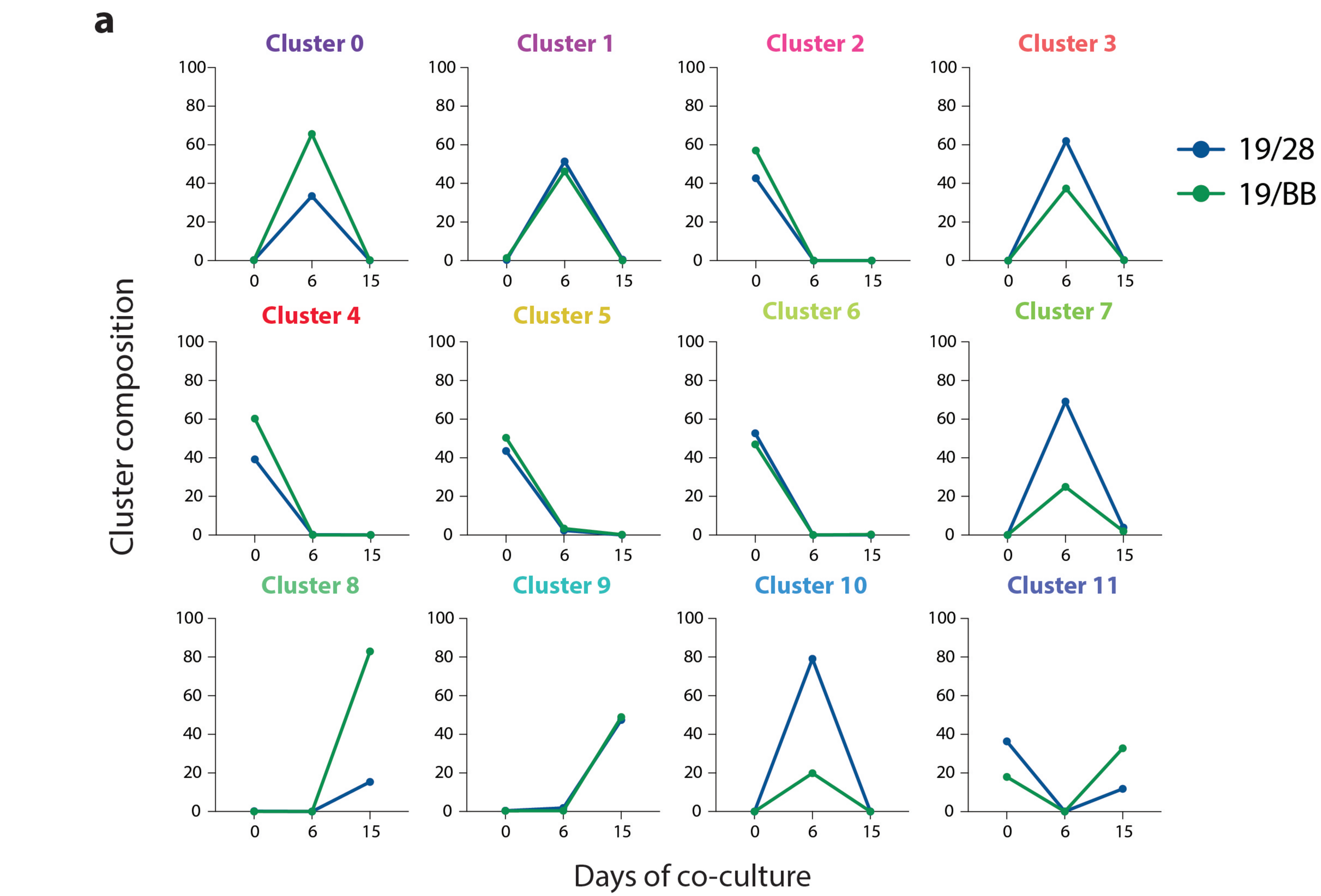

Supplementary Figure 4

a

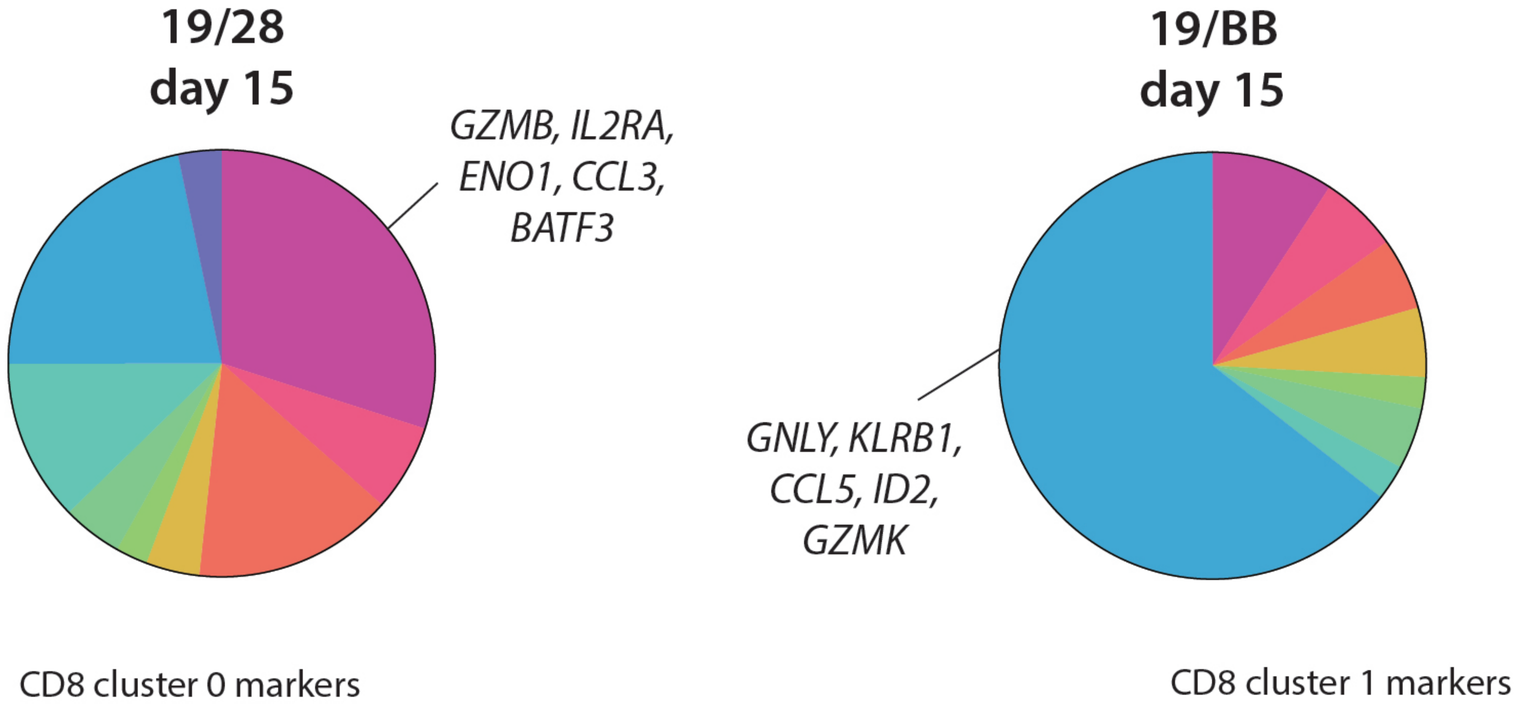

Supplementary Figure 5

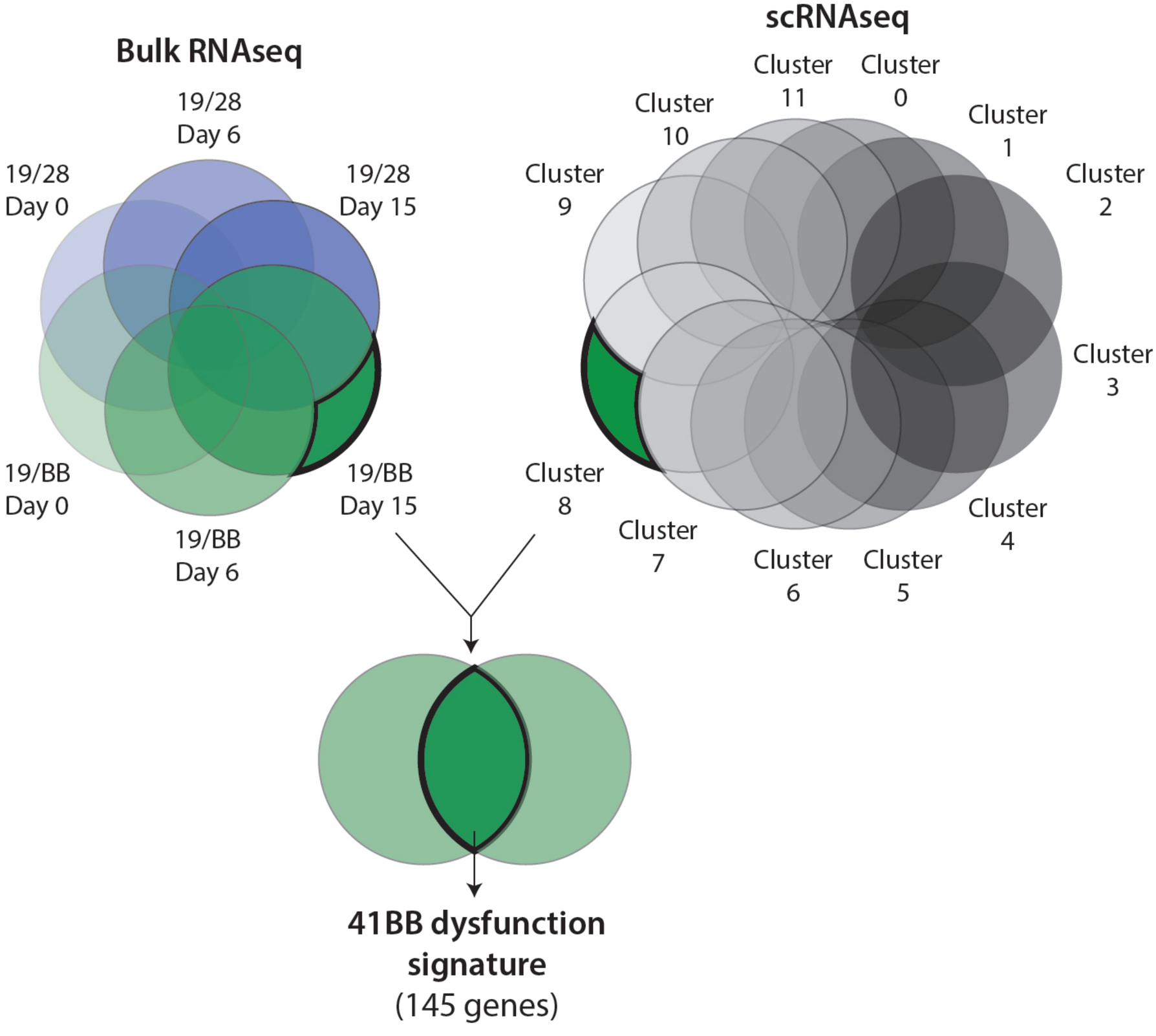

Supplementary Figure 6

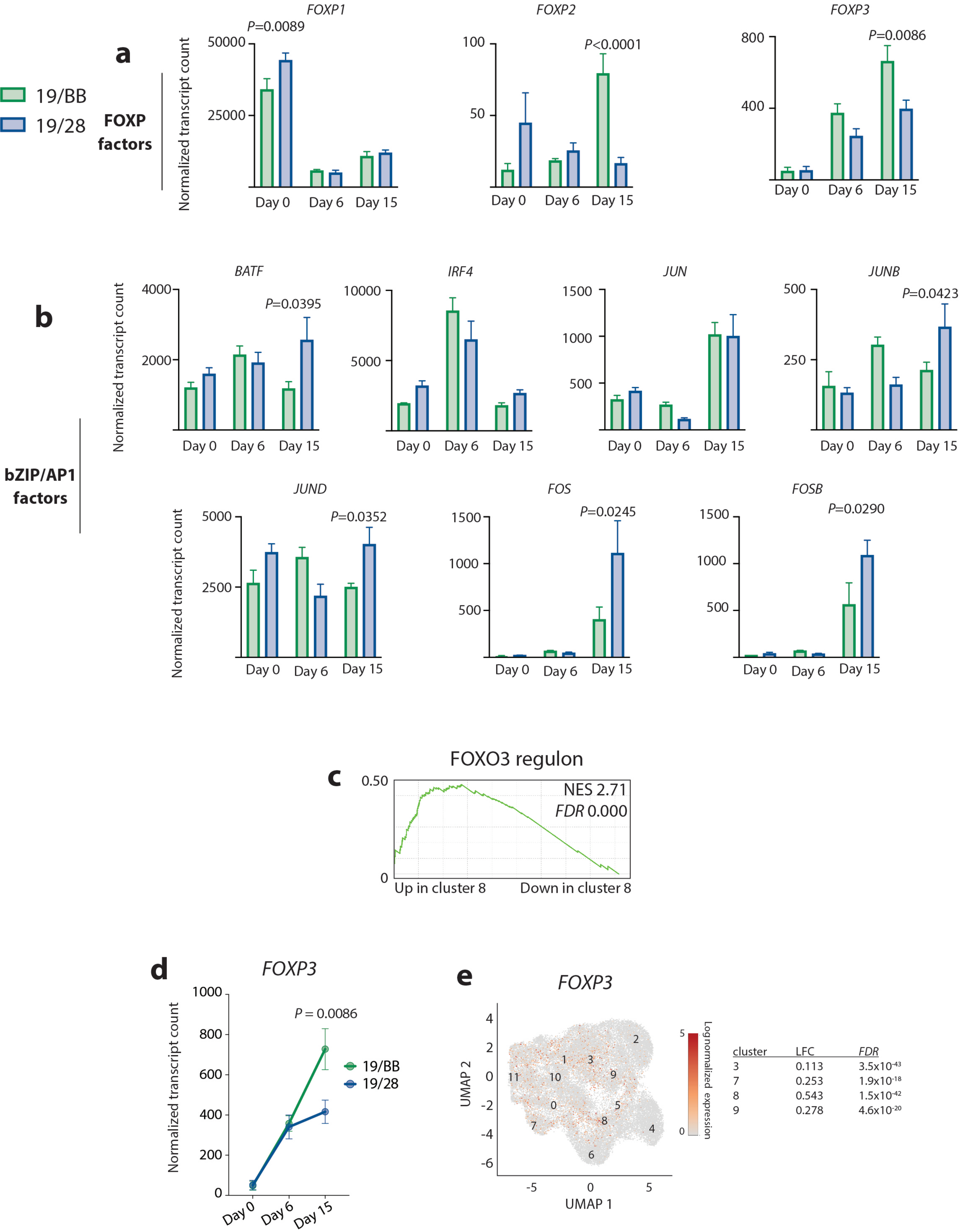

Supplementary Figure 7

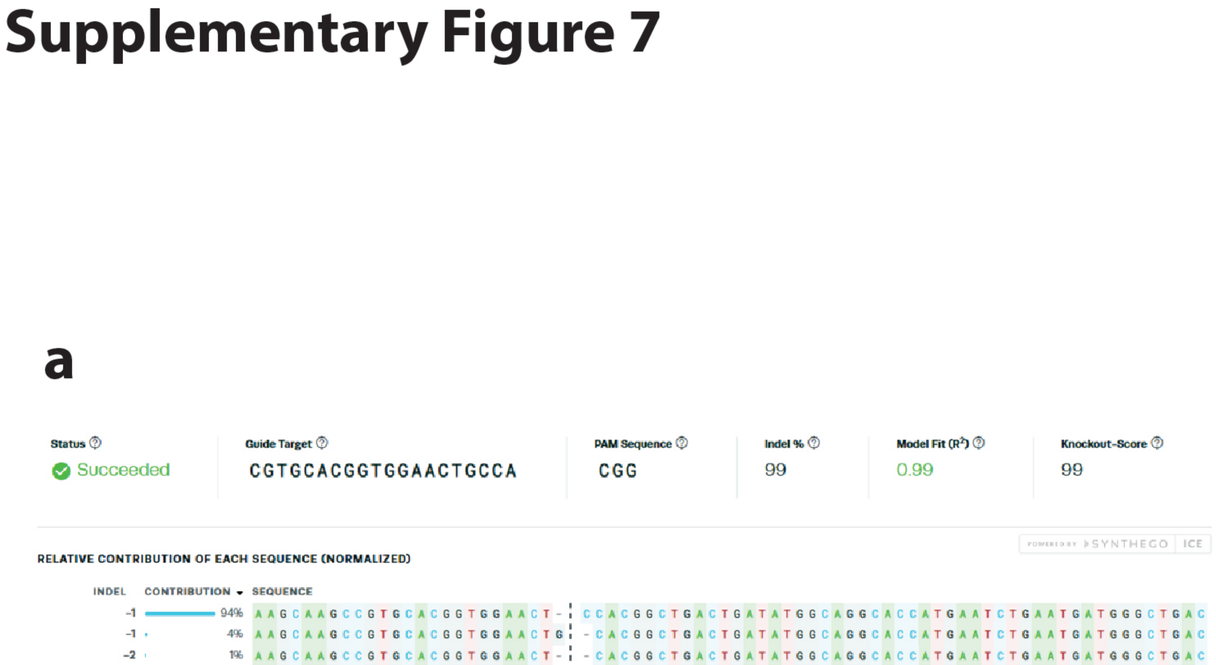

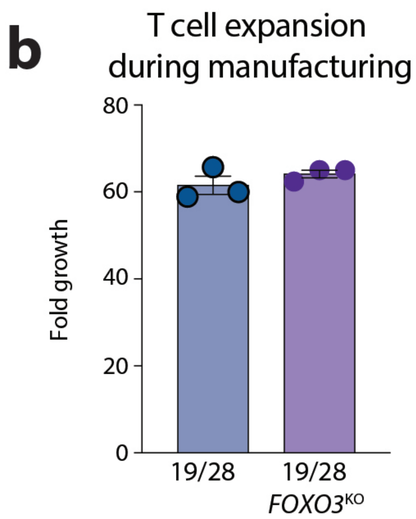

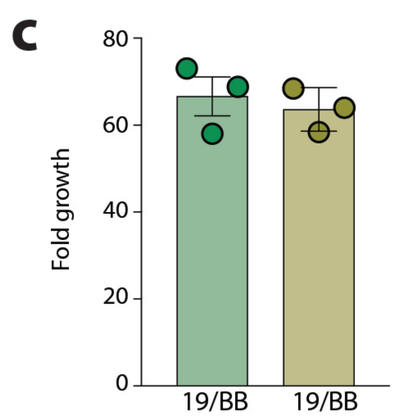

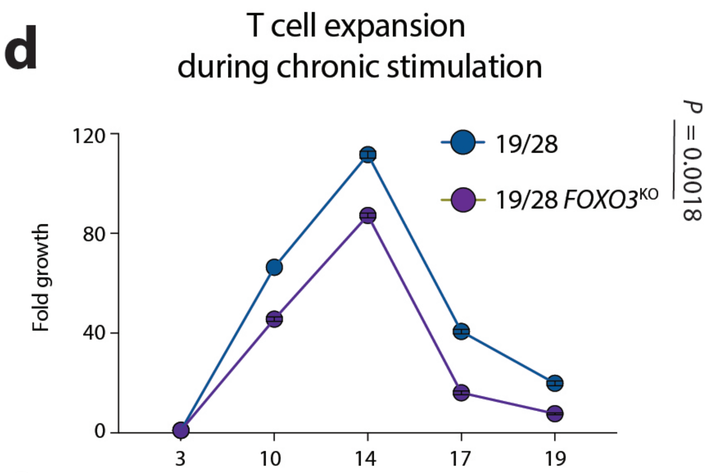

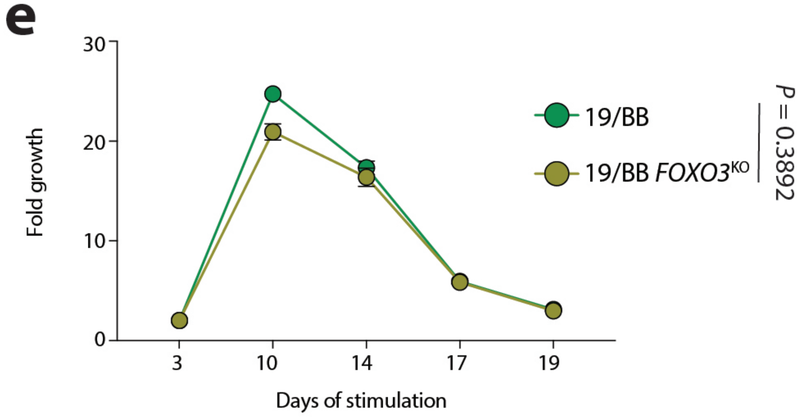

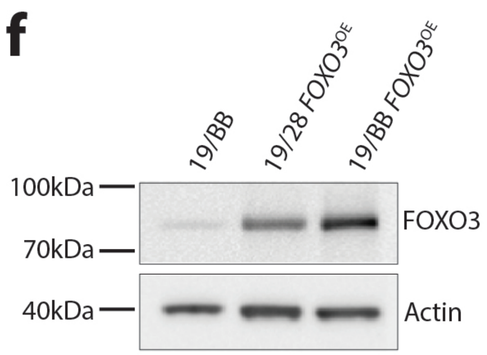

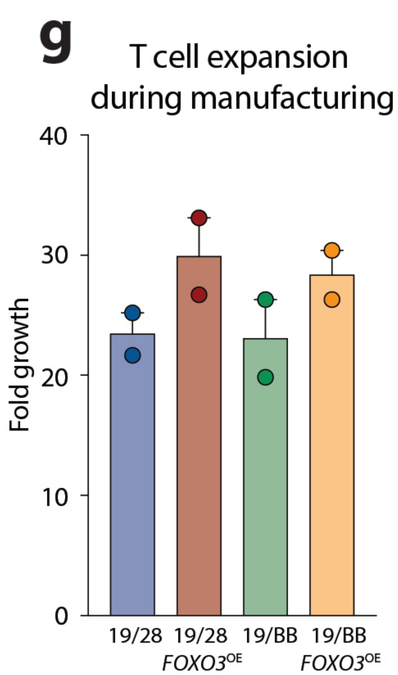

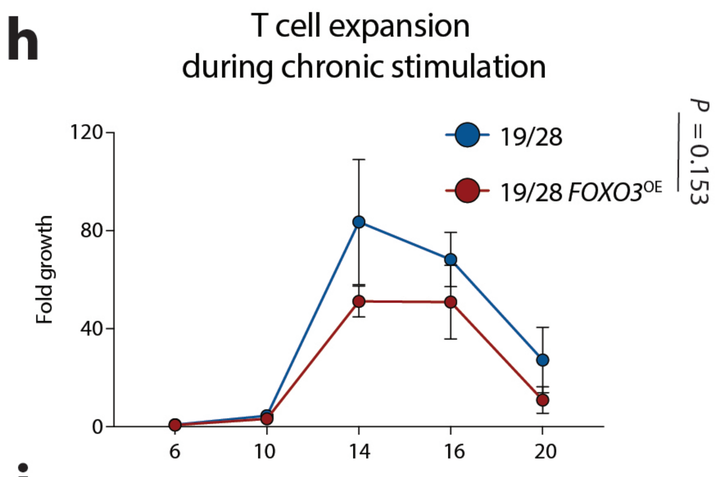

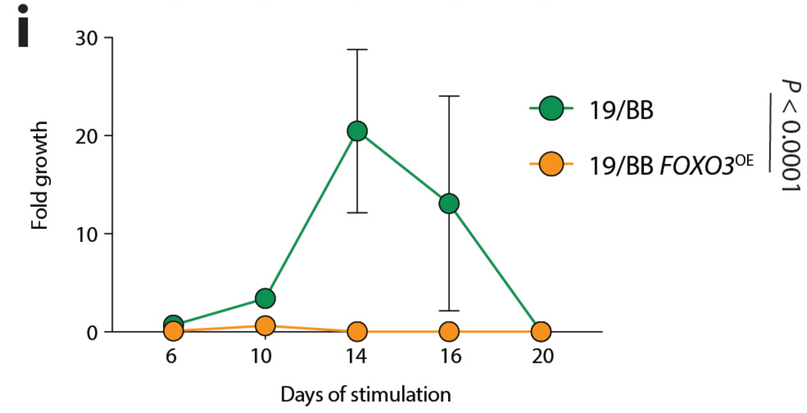

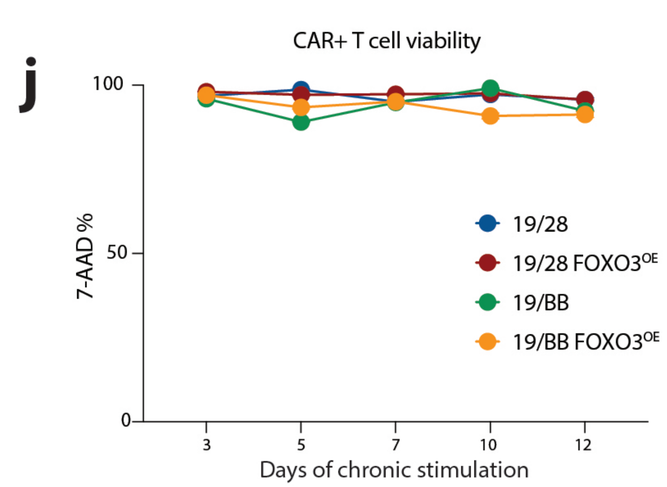

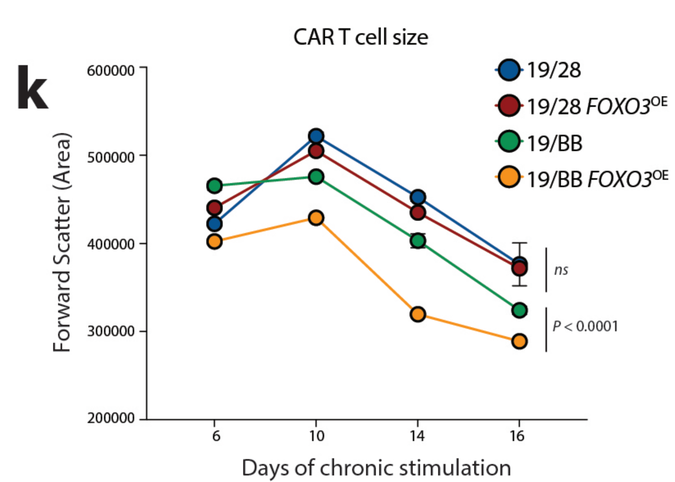

Supplementary Figure 8

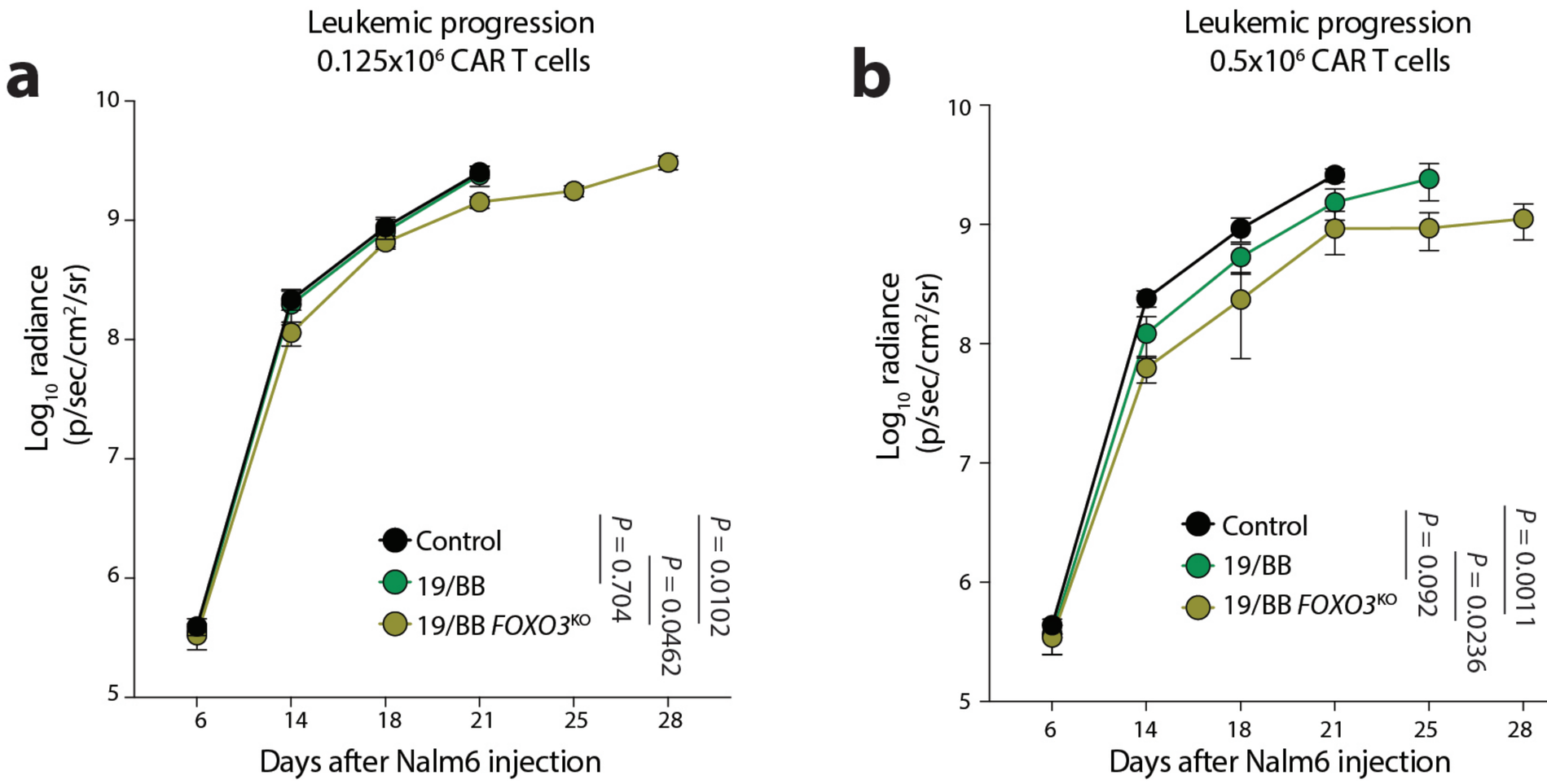

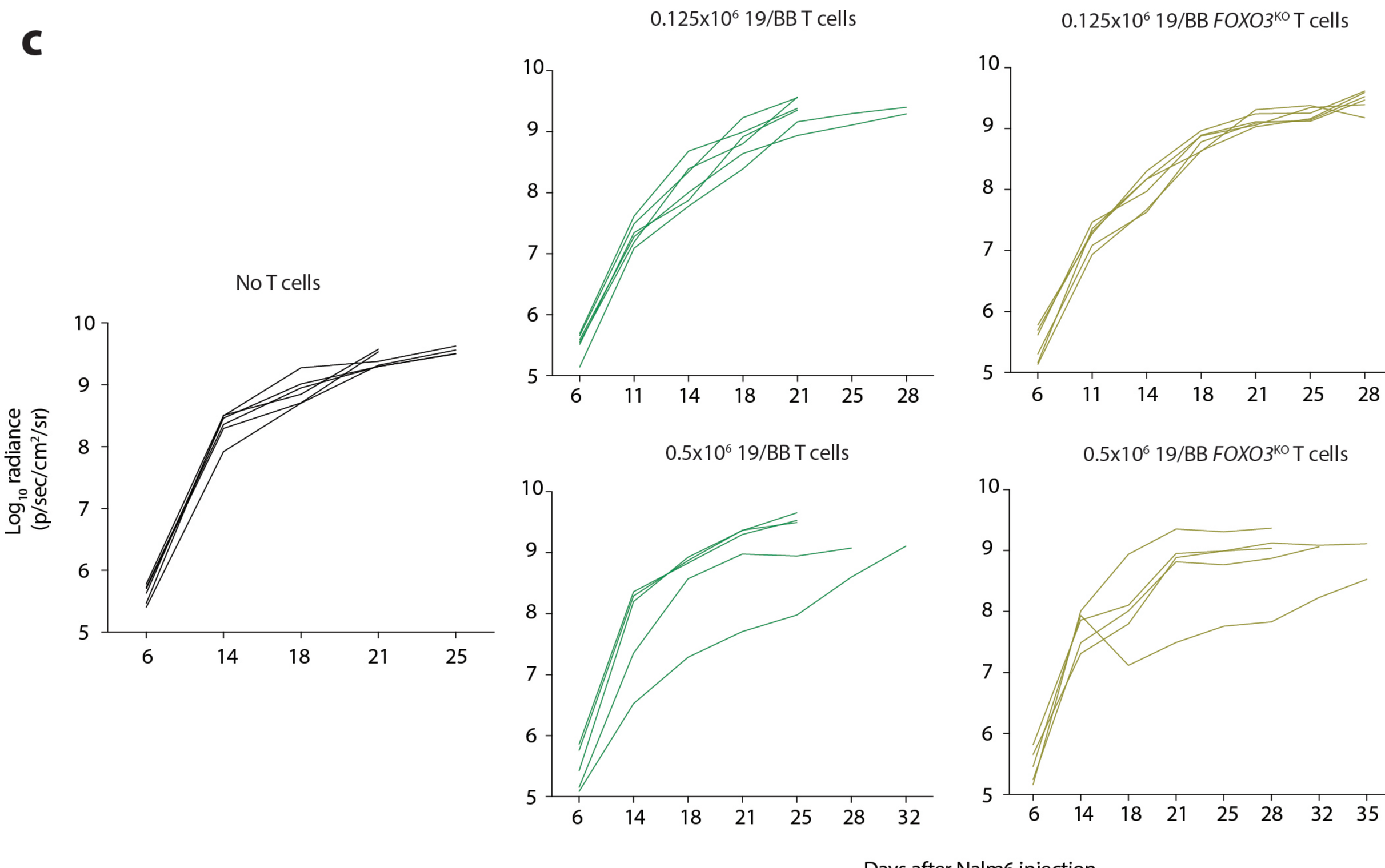

Supplementary Table 1: CyTOF panel

Target	Tag	Clone	Manufacturer	Catalog #
CD45	089Y	HI30	Fluidigm	3089003B
Ki-67	115In	8D5	Thermo	MA5-15690
CD3	141Pr	UCHT1	Fluidigm	3141019B
CD28	142Nd	CD28.2	biolegand	302902
CD45Ra	143Nd	H100	Fluidigm	3143006B
CD69	144Nd	FN50	Fluidigm	3144018B
CD4	145Nd	RPA-T4	Fluidigm	3145001B
CD8a	146Nd	RPA-T8	Fluidigm	3146001B
RORgt	147Sm	AFKJS-9	ebioscience	14-6988-82
CD278/ICOS	148Nd	C398.4A	Fluidigm	3148019B
CD56 (NCAM)	149Sm	NCAM16.2	Fluidigm	3155008B
CD223/LAG-3	150Nd	11C3C65	Fluidigm	3150030B
CD103	151Eu	Ber-ACT8	Fluidigm	3151011B
TCRgd	152Sm	11F2	Fluidigm	3152008B
CD62L	153Eu	DREG56	Fluidigm	3153004B
TIM3	154Sm	F38-2E2	Fluidigm	3154010B
CD27	155Gd	L128	Fluidigm	3158010B
CXCR3	156Gd	G025H7	Fluidigm	3156004B
CD134 (OX40)	158Gd	ACT35	Fluidigm	3158012B
CD197 (CCR7)	159Tb	G043H7	Fluidigm	3159003A
CD39	160Gd	A1	Fluidigm	3160004B
Tbet	161Dy	4B10	Fluidigm	3161014B
FoxP3	162Dy	PCH101	Fluidigm	3162011A
Eomes	163Dy	WD1928	ebioscience	14-4877-82
CD357 (GITR)	164Dy	621	biolegand	311602
CD45RO	165Ho	UCHL1	Fluidigm	3149001B
CD44	166Er	BJ18	Fluidigm	3166001B
Gata3	167Er	TWAJ	Fluidigm	3167007A
CD154 (CD40L)	168Er	24-31	Fluidigm	3168006B
CD25 (IL-2R)	169Tm	2A3	Fluidigm	3169003B
CTLA-4	170Er	14D3	Fluidigm	3170005B
Granzyme B	171Yb	GB11	Fluidigm	3171002B
CD38	172Yb	HIT2	Fluidigm	3172007B
CD137/4-1BB	173Yb	4B4-1	Fluidigm	3173015B
CD279 (PD-1)	174Yb	EH12.2H7	Fluidigm	3174020B
Perforin	175Lu	B-D48	Fluidigm	3175004B
CD127	176Yb	A019D5	Fluidigm	3176004B
TIGIT	209Bi	MBSA43	Fluidigm	3209013B

Supplementary Table 2: Human T cell exhaustion genesets

Li Cell 2019	Guo Nature Med 2018	Zheng Cell 2017	Zhang Nature 2018	Present in >2
ABI3	ACP5	ACP5	ACP5	ACP5
ADAM28	ALOX5AP	ADGRG1	AFAP1L2	AFAP1L2
AFAP1L2	ANXA5	AFAP1L2	ANXA5	AKAP5
AKAP5	APOBEC3C	AKAP5	APOBEC3C	ANXA5
ANAPC1P1	ATP6V1C2	BST2	APOBEC3G	APOBEC3C
ANLN	BHLHE40-AS1	CCL3	BATF	BST2
AOAH	BST2	CCND2	BST2	CCL3
APOBEC3B	BTLA	CD27	CCL3	CCL4
ASF1B	CCL3	CD27-AS1	CCL4	CCL4L1
ASPM	CCL4	CD2BP2	CCL4L1	CCND2
ATP8B4	CCND2	CD38	CCR1	CCR1
AURKB	CD200	CD63	CD27	CD200
BIRC5	CD27	CHST12	CD27-AS1	CD27
BTBD16	CD27-AS1	CREM	CD38	CD27-AS1
BUB1	CD38	CSF1	CD63	CD38
BUB1B	CD63	CTLA4	CD82	CD63
C16orf45	CD7	CTSD	COX5A	CD82
C2orf48	CD82	CXCL13	CTLA4	COX5A
CADM1	CDK2AP2	CXCR6	CTSD	CSF1
CCL3	CKS2	DFNB31	CTSW	CTLA4
CCL3L1	COTL1	DUSP4	CXCL13	CTSD
CCL3L3	COX5A	ENTPD1	CXCR6	CTSW
CCL4	CREG1	ENTPD1-AS1	DUSP4	CXCL13
CCL4L1	CTLA4	FKBP1A	ENTPD1	CXCR6
CCL5	CTSD	FUT8	FASLG	DUSP4
CCNB1	CXCL13	GALM	FKBP1A	ENTPD1
CCNB2	CXCR6	GZMB	FKBP1A-SDCBP2	FASLG
CCR1	DDIT4	HAVCR2	FUT8	FKBP1A
CD200	DNPH1	HLA-DMA	GSTO1	FKBP1A-SDCBP2
CD244	DTHD1	HLA-DRA	GZMB	FUT8
CD248	DUSP4	HMGN3	GZMH	GALM
CD38	DYNLL1	ICOS	HAVCR2	GZMB
CD63	ENTPD1	ID3	HLA-DQA1	GZMH
CD8A	FABP5	IFI35	HLA-DQB1	HAVCR2
CD8B	FASLG	IFNG	HLA-DRA	HLA-DMA
CD9	FKBP1A	IGFLR1	HLA-DRB1	HLA-DQA1
CDC20	FKBP1A-SDCBP2	IL2RB	HLA-DRB5	HLA-DRA
CDC45	FKBP5	ITGAE	HLA-DRB6	HLA-DRB1
CDC6	GALM	ITM2A	IFI27L2	HLA-DRB5
CDCA2	GPR25	LAG3	IFI6	HLA-DRB6
CDCA3	GZMB	LAYN	IFNG	ID3
CDCA5	HAVCR2	LINC00299	IGFLR1	IFI35

CDCA8	HLA-DRA	LYST	ISG15	IFNG
CDK1	HLA-DRB5	MIR155HG	ITGAE	IGFLR1
CDKN3	HLA-DRB6	MIR4632	ITM2A	ISG15
CDT1	HMGN1	MS4A6A	LAG3	ITGAE
CENPA	ID2	MTHFD1	MIR155	ITM2A
CENPW	IDH2	MTHFD2	MIR155HG	KRT81
CEP55	IFI35	MYO1E	MIR497HG	KRT86
CKAP2L	IFNG	MYO7A	MYO7A	LAG3
CLEC12A	IGFLR1	NAB1	NAB1	LAYN
CLIC3	IL21	NDFIP2	NDFIP2	LINC00299
CLNK	IL6ST	PARK7	PARK7	MIR155
CLSPN	ISG15	PDCD1	PDCD1	MIR155HG
CRTAM	ITGAE	PHLDA1	PHLDA1	MIR4632
CSF1	ITM2A	PKM	PKM	MIR497HG
CST7	ITPR1	PRDM1	PTTG1	MTHFD2
CTSW	KRT81	PRDX5	RBPJ	MYO1E
CXCL13	KRT86	PRF1	SIRPG	MYO7A
CXXC5	LAG3	PRKAR1A	SIT1	NAB1
DBN1	LAYN	RAB27A	SNAP47	NDFIP2
DEPDC1B	LIMS1	RALGDS	TIGIT	PARK7
DIAPH3	LINC00892	RGS1	TNFRSF18	PDCD1
DLGAP5	LRMP	RGS2	TNFRSF9	PHLDA1
DMC1	MIR155	SARDH	TNFSF4	PKM
DRAXIN	MIR155HG	SIRPG	TNIP3	PRDX5
DSCC1	MIR3917	SNAP47	TOX	PRF1
DTL	MIR4632	SNX9	VCAM1	PTTG1
E2F8	MIR497HG	STAT3		RAB27A
EGR2	MTHFD2	SYNGR2		RBPJ
ENTPD1	MYO7A	TIGIT		RGS1
EOMES	NAP1L4	TNFRSF1B		RGS2
ESCO2	NDFIP2	TNFRSF9		SARDH
ETV1	NR3C1	TOX		SIRPG
EXO1	PARK7	TPI1		SIT1
FAM111B	PDCD1	TRAFD1		SNAP47
FAM166B	PDIA6	UBE2F		SNX9
FAM3C	PHLDA1	UBE2F-SCLY		STMN1
FAM49A	PRDX3	VAPA		SYNGR2
FASLG	PRDX5	VCAM1		TIGIT
FBXO43	PSMB3	WARS		TNFRSF18
FCGR3A	PSMC3	YARS		TNFRSF9
FCRL3	PSMD4			TNFSF4
FXYD2	PSMD8			TNIP3
FXYD6-FXYD2	PTPN13			TOX
GABARAPL1	PTTG1			TPI1
GCNT1	RAB27A			VCAM1

GEM
GFOD1
GGH
GINS1
GINS2
GNG4
GNGT2
GNLY
GOLIM4
GPA33
GTSE1
GZMA
GZMB
GZMH
HAVCR2
HIST1H1B
HIST1H2AL
HJURP
HLA-DMA
HLA-DQA1
HLA-DQA2
HLA-DRB1
HLA-DRB6
HMMR
HMOX1
ID3
IFITM10
IFNG
IGFBP6
IRF8
ITGA1
ITGA2
ITGAE
ITM2C
KIF14
KIF15
KIF18B
KIF23
KIF2C
KIF4A
KIR2DL3
KIR2DL4
KLRC1
KLRC2
KLRC3
RANBP1
RBPJ
RGS1
RGS2
RNF19A
SAMSN1
SARDH
SIRPG
SIT1
SMCO4
SNAP47
SNRPB
SNX9
SRGN
STMN1
STRA13
SYNGR2
TIGIT
TMEM243
TNFRSF18
TNFRSF1B
TNFRSF9
TNFSF8
TNIP3
TOX
TPI1
UBE2L6
VCAM1
YWHAQ
ZBED2
ZBED2

KLRC4
KLRC4-KLRK1
KLRD1
KLRK1
KRT81
KRT86
LAG3
LAYN
LILRB1
LILRP2
LIMK1
LINC00158
LINC00299
LRRC28
MCM10
MCM2
MCM4
MELK
MKI67
MND1
MTFR2
MYBL2
MYO1E
MYO7A
NCAPG
NCR1
NEIL3
NEK2
NHS
NKG7
NUF2
ORC1
ORC6
P2RY1
PBK
PDLIM4
PHEX
PHGDH
PHLDA1
PIK3AP1
PIK3R6
PKMYT1
PLCG2
PLK1
POC1A

POLQ
PON2
PON3
PRF1
PROX2
PRR11
PRSS30P
PTGIS
PTMS
PTPRK
QPRT
RAD51
RAD51AP1
RDH10
REEP2
REG4
RGS13
RRM2
SEMA4A
SFTPB
SHCBP1
SKA1
SKA3
SLAMF7
SLC17A9
SLC2A8
SLC43A3
SMIM10
SPAG5
SPC24
SPC25
SPRY1
SPRY2
STMN1
STYK1
SYNGR1
TIGIT
TIMD4
TK1
TMEM155
TNFRSF9
TNFSF4
TNFSF9
TNIP3
TNS3

TOP2A
TPX2
TRIP13
TROAP
TSPAN13
TTC24
TTK
TYMS
UBE2C
UBE2T
UHRF1
VCAM1
WDHD1
WIPF3
XCL2
XRCC2
YBX3
ZBED2
ZBTB32
ZC3H12C
ZNF683
ZWINT

Present in all 4
CCL3
CSF1
CTLA4
CXCL13
CXCR6
HAVRC2
IFNG
ITGAE
LAG3
LYST
MYO7A
PDCD1
PHLDA1
RAB27A
SNAP47
TNFRSF1B
TNFRSF9

Supplementary Table 3: Dysfunctional 41BB-based CAR T cell (Tbbd) gene signature of dysfu

ABCG1
ADAM8
AHI1
AKNA
ALOX5AP
ANKRD12
ANKRD28
AOAH
ARHGAP9
ARHGEF12
ASB2
ATP8B4
BCL2L11
CAMK4
CBLB
CCL5
CCR8
CD2
CD27
CD37
CD3D
CD52
CD63
CD69
CD8A
CD8B
CD96
CDKN1B
CFLAR
CLEC2B
CLEC2D
CLSTN3
CST7
CTSW
CXCR6
CYTH4
DAPK2
DDHD1
DDX17
DOCK8
DUSP1
ELF1
ENTPD1

ERN1
EVA1B
EVI2B
EVL
FASLG
FCER1G
FYB1
GABARAPL1
GADD45B
GCNT1
GLIPR1
GNLY
GOLGA8A
GOLGA8B
GPR171
GPR174
GZMK
HAVCR2
HCST
HOPX
HSH2D
ID2
IER5L
IGFLR1
IKZF2
IL10RA
IL16
IL2RG
IL9R
INPP5D
ITGA1
ITGAX
JAK3
JAML
JUN
KDM5B
KIT
KLF6
KLRB1
KLRC2
KLRC3
KLRC4
KLRD1
KLRK1
KMT2E

LNPEP
LRRC28
LYST
MCL1
MCTP2
MEF2A
NBL1
NCAM1
NCF4
NCR3
NELL2
NFATC3
NLRC3
NT5E
OGT
PAG1
PDCD4
PDE3B
PDE7A
PDE7B
PGGHG
PLAAT4
PPP1R15A
PRF1
PRKCA
PTGER4
PTPN22
RAB24
RAB37
RASGRP1
RBM39
RBPJ
REG4
RESF1
RIN3
RPS6KA3
SCLY
SERPINE1
SIRPG
SKAP1
SLAMF7
SLC1A4
SMAD3
SRGAP3
SYTL2

TGFB1
THEMIS
TMX4
TNFAIP3
TSC22D3
TSPAN32
TTN
TXNIP
XAF1
XCL1
YPEL3
ZNF217

nction